ChemComm

Chemical Communications

rsc.li/chemcomm
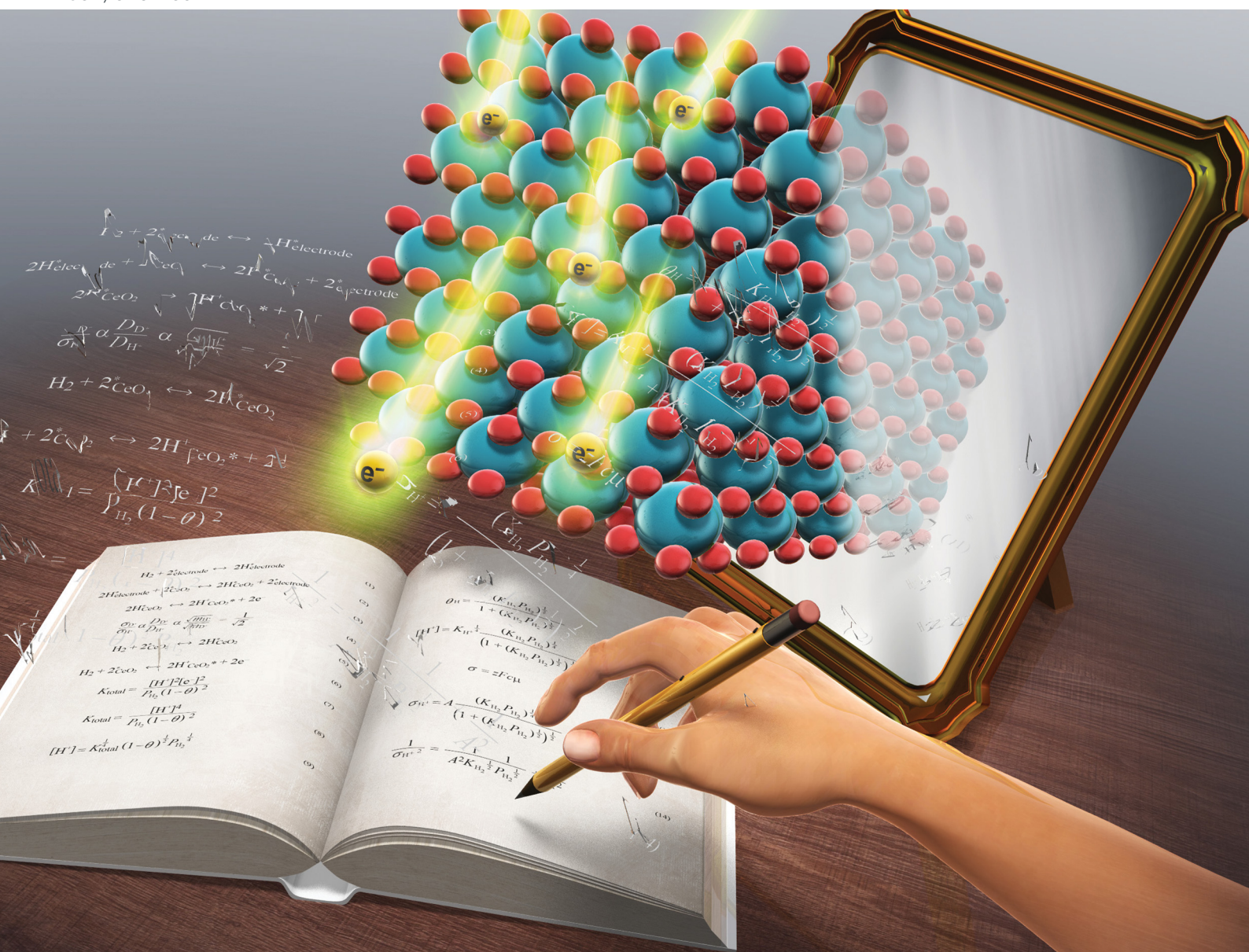
ROYAL SOCIETY
OF CHEMISTRY

COMMUNICATION
Yasushi Sekine *et al.*
Quantitative investigation of CeO$_2$ surface proton
conduction in H$_2$ atmosphere

Check for updates

Quantitative investigation of CeO$_2$ surface proton conduction in H$_2$ atmosphere†

Taku Matsuda, Ryo Ishibashi, Yoshiki Koshizuka, Hideaki Tsuneki and Yasushi Sekine [ID] *

This report is the first describing a study quantitatively analysing aspects of oxide surface protonics in a dry H$_2$ atmosphere. Elucidating surface protonics is important for electrochemical and catalytic applications. In this study, AC impedance spectroscopy was used to investigate surface conduction properties of porous CeO$_2$ at low temperatures (423–573 K) and in a dry H$_2$ atmosphere. Results demonstrated that the conductivity increased by several orders of magnitude when H$_2$ was supplied. Dissociative adsorption of H$_2$ contributes to conduction by forming proton–electron pairs. Also, H/D isotope exchange studies confirmed protons as the dominant conduction carriers. Furthermore, H$_2$ adsorption equilibrium modelling based on the Langmuir mechanism was applied to explain the H$_2$ partial pressure dependence of conductivity. For the first time, the obtained model explains the experimentally obtained results both qualitatively and quantitatively. These findings represent new insights into surface protonics in H$_2$ atmosphere.

The phenomenon of surface protonics has potential applications in proton-conducting fuel cells,[1] proton exchange membranes[2] and electrochemical gas sensors.[3] This phenomenon is defined as proton transfer at oxide surfaces. Moreover, surface protonics plays an important role in heterogeneous catalysis.[4–17] Surface proton conduction is observed in the presence of H$_2$O or H$_2$ at temperatures of room temperature to 773 K.[18–31] Because adsorption plays an important role, porous samples at low temperatures are preferred; for H$_2$O adsorption, multilayers are formed. It is noteworthy that no multilayer is formed in the adsorption of H$_2$, thereby leading to a difference in surface proton transport behaviour: in an H$_2$O atmosphere, free protons and mainly hydronium ions move through the chemisorbed and physisorbed water layers on the oxide, respectively according to the Grotthuss and vehicle mechanisms.[29] Which mechanism prevails depends on the water layer thickness in relation to temperature and

Department of Applied Chemistry, Waseda University, 3-4-1, Okubo, Shinjuku, Tokyo, 169-8555, Japan. E-mail: ysekine@waseda.jp

† Electronic supplementary information (ESI) available. See DOI: https://doi.org/10.1039/d2cc03687h

relative humidity.[29] However, in an H$_2$ atmosphere, dissociative adsorption of H$_2$ produces proton–electron pairs. The produced protons are transferred on the surface lattice oxygen by a hopping mechanism.[31] The presence of a metal (*e.g.* Pt) is regarded as necessary for H$_2$ dissociation and spillover.

The evaluation of surface proton conduction is of great importance. For that evaluation, AC impedance spectroscopy is a promising technique because it allows separation of the electrical properties into components (*e.g.* bulk and grain boundaries), and facilitates their subsequent quantified. To date, many reports have described studies using AC impedance measurements to characterise surface proton conduction properties in an H$_2$O atmosphere.[18–30] Earlier reports described that surface proton conductivity under an H$_2$O atmosphere can be quantified using an equivalent circuit suitable for the analysis.[28–30] The equivalent circuit included surface components parallel to the bulk and grain boundary components, thereby allowing direct assessment of surface proton transport in the adsorbed water layer.

However, the evaluation of surface proton conduction under a dry H$_2$ atmosphere has been reported only qualitatively.[31] It has not yet reached the stage of quantitative evaluation. Therefore, a more general theory of surface proton conduction under a dry H$_2$ atmosphere must be found.

This study investigated surface proton conduction properties induced by dry H$_2$ supply on porous CeO$_2$ by AC impedance measurements. Then a model was proposed to interpret those properties in terms of H$_2$ partial pressure dependence. This study provides new insights into surface proton conduction in H$_2$ atmosphere on an oxide surface. As the sample to be measured, we selected CeO$_2$ (JRC-CEO-1), because surface protonic transport on CeO$_2$ has been widely studied[25–28] and CeO$_2$ as a surface proton-conducting oxide is important for catalysis and fuel cell applications.[4–12,27] Experimental procedures are described in ESI.†

First, the H$_2$ supply effects on conductivity for porous CeO$_2$ were investigated at various temperatures by AC impedance measurement. The obtained data were analysed using a parallel
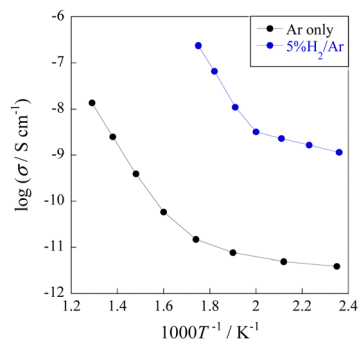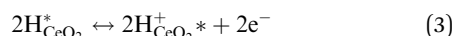
Fig. 1 Temperature dependence of conductivity for CeO₂ under Ar and 5%H₂/Ar atmospheres.

RQ equivalent circuit presented in Fig. S1 (ESI†). The temperature dependence of the CeO₂ conductivity with and without H₂ supply is presented in Fig. 1. From these data, we inferred that the H₂ supply increased the conductivity by several orders of magnitude. The marked increase in conductivity is not attributable to oxygen vacancy formation, as explained in the discussion of ESI† (see Fig. S2 and S3). A change in the activation energy was also observed before and after H₂ supply, as shown in Table 1, suggesting a change in the conduction mechanism or conductive carriers. According to earlier reports, porous samples with relative density of around 60% provide information related to conduction with adsorbed species.[28,31] As shown in Fig. S4 in ESI,† SEM observations confirmed the presence of numerous pores in samples with relative density of approximately 60%.

The increase in conductivity can therefore be attributed to the dissociative adsorption of H₂ and the formation of conducting species, as presented in eqn (1)–(3).

$$H_2 + 2^*_{electrode} \leftrightarrow 2H^*_{electrode} \tag{1}$$

$$2H^*_{electrode} + 2^*_{CeO_2} \leftrightarrow 2H^*_{CeO_2} + 2^*_{electrode} \tag{2}$$

$$2H^*_{CeO_2} \leftrightarrow 2H^+_{CeO_2}* + 2e^- \tag{3}$$

Therein, * denotes adsorption site. Hydrogen spillover has been reported earlier.[32,33]

Dissociative adsorption of H₂ is thought to have occurred on the Pt electrode. It then spilled over onto CeO₂, giving rise to proton and electron pairs. On various reducible oxides (*e.g.* CeO₂, TiO₂, WO₃), protons are said to bind to surface lattice oxygen; electrons reduce metal cations near O–H bonds.[34] Protons move over the oxide surface, whereas electrons move *via* the conduction band.

Table 1 Apparent activation energy of conduction for each condition

Condition (—)	Activation energy (eV)
Ar only (>573 K)	1.33
Ar only (<573 K)	0.18
5%H₂/Ar (>500 K)	1.48
5%H₂/Ar (<500 K)	0.24

Table 2 H/D isotope effects on conductivity at each temperature

Temp (K)	σ_D/σ_H (—)
573	0.79
548	0.67
523	0.59
498	0.72
473	0.69
448	0.68
423	0.69

Next, the H/D isotope effect was investigated to identify the dominant conducting carrier in the H₂ atmosphere. As a result, the H/D isotope effect was identified at each measured temperature, as shown in Table 2 and in Fig. S5 in ESI.† Those findings are explainable by the different barriers posed by the hopping mechanism against the transfer of protons and deuterons. The deuteron transfer barrier is well known to be higher than the proton transfer barrier because of the different energies of the O–H and O–D ground states. According to classical theory, the theoretical value of the H/D isotope effect on the hopping proton/deuteron conductivity $\sigma_{D^+}/\sigma_{H^+}$ is expected to be $\frac{1}{\sqrt{2}}$ ($\fallingdotseq 0.71$),[35,36] as calculated using the following equation.[37]

$$\frac{\sigma_{D^+}}{\sigma_{H^+}} \propto \frac{D_{D^+}}{D_{H^+}} \propto \frac{\sqrt{m_{H^+}}}{\sqrt{m_{D^+}}} = \frac{1}{\sqrt{2}} \tag{4}$$

In that equation, D denotes diffusivity; m stands for the mass of the diffusing species. As Table 2 shows, the theoretical value closely approximates the experimentally obtained values. It can therefore be inferred that protons are the dominant conduction carrier in the H₂ atmosphere and that they are transferred *via* the hopping mechanism. The possibility of proton conduction in the bulk was ruled out; in general, the diffusivity of hydrogen in CeO₂ is low,[38] and considerably high temperatures (above 1050 K) are required for CeO₂ to exhibit the bulk proton conduction.[39] So we attributed the measured proton conductivity only to the oxide surface and not to the bulk.

Next, to elucidate the surface protonics in an H₂ atmosphere further, the effects of the H₂ partial pressure dependence were investigated. As Fig. 2 shows, the conductivity increased
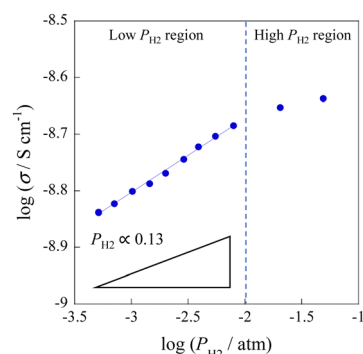

Fig. 2 H₂ partial pressure dependence of conductivity for CeO₂ at 473 K.

concomitantly with increasing H_2 partial pressure. At the low H_2 partial pressure region, the slope was 0.13. It then saturated gradually with increasing H_2 partial pressure, indicating a relation between conductivity and H_2 coverage. Based on these results, an H_2 adsorption equilibrium model was proposed to interpret the H_2 partial pressure dependence of conductivity.

As explained in the preceding section, dissociative adsorption of H_2 and spillover lead to the formation of protons on the CeO_2 surface, as shown particularly by eqn (1)–(3). For simplicity, eqn (1) and (2) were combined. The reaction on the Pt electrode was omitted.

$$H_2 + 2^*_{CeO_2} \leftrightarrow 2H^*_{CeO_2} \tag{5}$$
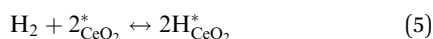
The total equation for eqn (3) and (5) and the equilibrium constant K_{total} can be written as

$$H_2 + 2^*_{CeO_2} \leftrightarrow 2H^+_{CeO_2}* + 2e^- \tag{6}$$
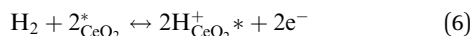
$$K_{total} = \frac{[H^+]^2[e^-]^2}{P_{H_2}(1-\theta)^2} \tag{7}$$

where θ denotes the coverage over CeO_2. Considering charge neutrality ($[H^+] = [e^-]$), the following equation is obtainable.

$$K_{total} = \frac{[H^+]^4}{P_{H_2}(1-\theta)^2} \tag{8}$$

Then, rearranging eqn (8) yields the following equation.

$$[H^+] = K_{total}^{\frac{1}{4}}(1-\theta)^{\frac{1}{2}}P_{H_2}^{\frac{1}{4}} \tag{9}$$

This equation represents the H_2 partial pressure dependence of proton concentration. However, the relation between H_2 partial pressure and coverage is not considered. The H_2 partial pressure dependence is explainable by the Langmuir adsorption model. The Langmuir adsorption model includes the assumption that the adsorption sites are homogeneous without interactions and that no interaction exists between neighbouring adsorbed molecules. The model also describes the adsorption of molecules on a solid surface as a function of gas pressure at a constant temperature. Applying the Langmuir adsorption model to eqn (5) gives the following equation.

$$\theta_H = \frac{(K_{H_2}P_{H_2})^{\frac{1}{2}}}{1 + (K_{H_2}P_{H_2})^{\frac{1}{2}}} \tag{10}$$

Therein, K_{H_2} denotes the Langmuir adsorption constant. The H_2 atom coverage represented in the eqn (10) can be assumed to be similar to θ. Then, substituting the coverage in the eqn (9) yields the following equation.

$$[H^+] = K_{H^+}^{\frac{1}{4}}\frac{(K_{H_2}P_{H_2})^{\frac{1}{4}}}{\left(1 + (K_{H_2}P_{H_2})^{\frac{1}{2}}\right)^{\frac{1}{2}}} \tag{11}$$

In that equation, K_{H^+} is the equilibrium constant for eqn (5). The carrier concentration such as that of protons is related to the conductivity.

$$\sigma = zFc\mu \tag{12}$$

Therein, z, F, c, and μ respectively denote the charge number, Faraday's constant, carrier concentration, and mobility.

Substituting the proton concentration expressed in eqn (11) into eqn (12) yields the following equation.

$$\sigma_{H^+} = A\frac{(K_{H_2}P_{H_2})^{\frac{1}{4}}}{\left(1 + (K_{H_2}P_{H_2})^{\frac{1}{2}}\right)^{\frac{1}{2}}} \tag{13}$$

In this equation, $A = F\mu_{H^+}K_{H^+}^{\frac{1}{4}}$

Therefore, the following can be inferred from eqn (13); (1) At low H_2 partial pressures, $(K_{H_2}P_{H_2})^{\frac{1}{2}} \ll 1$. Then the proton conductivity is proportional to the power of 1/4 of the H_2 pressure. (2) At high H_2 partial pressures, $(K_{H_2}P_{H_2})^{\frac{1}{2}} \gg 1$. Then the proton conductivity is independent of the H_2 partial pressure. These conclusions show close agreement with the experimentally obtained results. Furthermore, to explain the dependence of conductivity on H_2 partial pressure quantitatively rather than qualitatively, eqn (13) can be rearranged as shown below.

$$\frac{1}{\sigma_{H^+}^2} = \frac{1}{A^2 K_{H_2}^{\frac{1}{2}}P_{H_2}^{\frac{1}{2}}} + \frac{1}{A^2} \tag{14}$$

The values of A and K_{H_2} are obtainable by the slope and intercept of $\frac{1}{\sigma_{H^+}^2}$ vs. $\frac{1}{P_{H_2}^{\frac{1}{2}}}$. The relation between $\frac{1}{\sigma_{H^+}^2}$ vs. $\frac{1}{P_{H_2}^{\frac{1}{2}}}$ is shown in Fig. 3.

As expected, a linear relation was confirmed. The values of A and K_{H_2} were calculated respectively as 2.5×10^{-9} S cm^{-1} and 4.8×10^2 atm^{-1}. Substituting these values in the eqn (13) enables calculation of the value of σ_{H^+} at the H_2 partial pressure. A comparison of the experimentally obtained data with the calculated data is presented in Fig. 4. The calculated σ_{H^+} showed good correspondence with the experimentally obtained results, thereby proving the model validity.

In summary, AC impedance measurements were taken to characterise the electrical properties of porous CeO_2 in a dry H_2 atmosphere. A marked increase in conductivity with H_2 supply was observed, suggesting the formation of conductive carriers
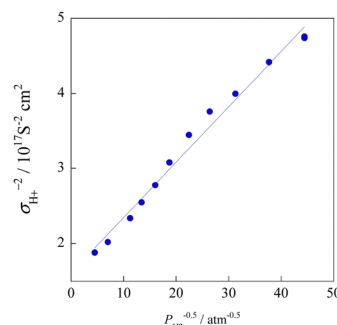

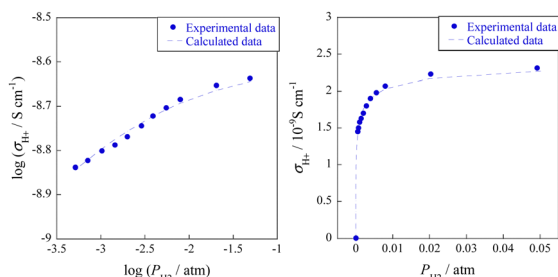**Fig. 3** Relation between $P_{H_2}^{-0.5}$ and $\sigma_{H^+}^{-2}$.

Fig. 4 H₂ partial pressure dependence of conductivity for CeO₂ at 473 K: experimentally obtained data and calculated data.
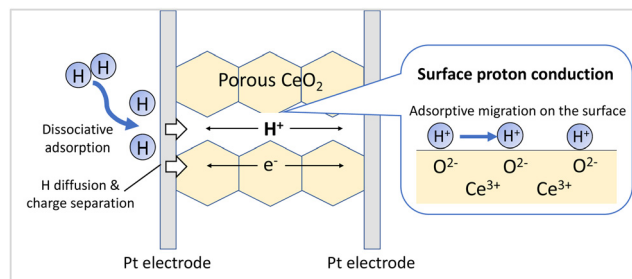

Fig. 5 Schematic image of the surface proton conduction in a dry H₂ condition on CeO₂.

(protons and electrons) by dissociative adsorption of H₂ as shown in Fig. 5. The H/D isotope effect was also observed, indicating protons as the dominant conductive carriers. Furthermore, the proposed H₂ adsorption equilibrium model quantitatively describes the H₂ partial pressure dependence of the conductivity. The model presented herein provides new insights into surface protonics in a dry H₂ atmosphere. The development of surface protonics in a dry H₂ atmosphere and the establishment of a method for measuring and evaluating such protonics are expected to be applied to various catalytic reactions such as ammonia synthesis in a dry H₂ atmosphere in the future.

Conflicts of interest

The authors have no conflicts of interest.

References

1 S. Kim, H. Park, M. Martin and Z. Munir, *Adv. Mater.*, 2008, **20**, 556–559.
2 A. Shabanikia, M. Javanbakht, H. Salar Amoli, K. Hooshyari and M. Enhessari, *J. Electrochem. Soc.*, 2014, **161**, 1403–1408.
3 M. Sakthivel and W. Weppner, *J. Phys. D: Appl. Phys.*, 2007, **40**, 7210–7216.
4 M. Torimoto, S. Ogo, Y. Hisai, N. Nakano, A. Takahashi, Q. Ma, J. G. Seo, H. Tsuneki, T. Norby and Y. Sekine, *RSC Adv.*, 2020, **10**, 26418–26424.
5 A. Takahashi, R. Inagaki, M. Torimoto, Y. Hisai, T. Matsuda, Q. Ma, J. G. Seo, T. Higo, H. Tsuneki, S. Ogo, T. Norby and Y. Sekine, *RSC Adv.*, 2020, **10**, 14487–14492.
6 K. Murakami, Y. Tanaka, R. Sakai, Y. Hisai, S. Hayashi, Y. Mizutani, T. Higo, S. Ogo, J. G. Seo, H. Tsuneki and Y. Sekine, *Chem. Commun.*, 2020, **56**, 3365–3368.
7 K. Yamada, S. Ogo, R. Yamano, T. Higo and Y. Sekine, *Chem. Lett.*, 2020, **49**(3), 303–306.
8 K. Takise, A. Sato, S. Ogo, J. G. Seo, K. Imagawa, S. Kado and Y. Sekine, *RSC Adv.*, 2019, **9**, 27743–27748.
9 M. Torimoto, K. Murakami and Y. Sekine, *Bull. Chem. Soc. Jpn.*, 2019, **92**(10), 1785–1792.
10 K. Takise, A. Sato, K. Murakami, S. Ogo, J. G. Seo, K. Imagawa, S. Kado and Y. Sekine, *RSC Adv.*, 2019, **9**, 5918–5924.
11 R. Inagaki, R. Manabe, Y. Hisai, Y. Kamite, T. Yabe, S. Ogo and Y. Sekine, *Int. J. Hydrogen Energy*, 2018, **43**(31), 14310–14318.
12 R. Manabe, S. Okada, R. Inagaki, K. Oshima, S. Ogo and Y. Sekine, *Sci. Rep.*, 2016, **6**, 38007.
13 M. Kosaka, T. Higo, S. Ogo, J. G. Seo, K. Imagawa, S. Kado and Y. Sekine, *Int. J. Hydrogen Energy*, 2020, **45**(1), 738–743.
14 T. Yabe, K. Yamada, K. Murakami, K. Toko, K. Ito, T. Higo, S. Ogo and Y. Sekine, *ACS Sustainable Chem. Eng.*, 2019, **7**(6), 5690–5697.
15 A. Gondo, R. Manabe, R. Sakai, K. Murakami, T. Yabe, S. Ogo, M. Ikeda, H. Tsuneki and Y. Sekine, *Catal. Lett.*, 2018, **148**(7), 1929–1938.
16 K. Murakami, R. Manabe, H. Nakatsubo, T. Yabe, S. Ogo and Y. Sekine, *Catal. Today*, 2018, **303**, 271–275.
17 R. Manabe, H. Nakatsubo, A. Gondo, K. Murakami, S. Ogo, H. Tsuneki, M. Ikeda, A. Ishikawa, H. Nakai and Y. Sekine, *Chem. Sci.*, 2017, **8**, 5434–5439.
18 S. Kim, H. J. Avila-Paredes, S. Wang, C. T. Chen, R. A. Souza, M. Martin and Z. A. Munir, *Phys. Chem. Chem. Phys.*, 2009, **11**, 3035–3038.
19 B. Scherrer, M. V. F. Schlupp, D. Stender, J. Martynczuk, J. G. Grolig, H. Ma, P. Kocher, T. Lippert, M. Prestat and L. J. Gauckler, *Adv. Funct. Mater.*, 2013, **23**, 1957–1964.
20 M. T. Colomer, *Adv. Mater.*, 2006, **18**, 371–374.
21 H. J. Avila-Paredes, J. Zhao, S. Wang, M. Pietrowski, R. A. de Souza, A. Reinholdt, Z. A. Munir, M. Martin and S. Kim, *J. Mater. Chem.*, 2010, **20**, 990–994.
22 S. Miyoshi, Y. Akao, N. Kuwata, J. Kawamura, Y. Oyama, T. Yagi and S. Yamaguchi, *Solid State Ionics*, 2012, **207**, 21–28.
23 S. Miyoshi, Y. Akao, N. Kuwata, J. Kawamura, Y. Oyama, T. Yagi and S. Yamaguchi, *Chem. Mater.*, 2014, **26**, 5194–5200.
24 R. Sato, S. Ohkuma, Y. Shibuta, F. Shimojo and S. Yamaguchi, *J. Phys. Chem. C*, 2015, **119**, 28925–28933.
25 G. Gregori, M. Shirpour and J. Maier, *Adv. Funct. Mater.*, 2013, **23**, 5861–5867.
26 M. Shirpour, G. Gregori, R. Merkle and J. Maier, *Phys. Chem. Chem. Phys.*, 2011, **13**, 937–940.
27 Y. Xing, Y. Wu, L. Li, Q. Shi, J. Shi and S. Yun, *ACS Energy Lett.*, 2019, **4**, 2601–2607.
28 R. Manabe, S. Ø. Stub, T. Norby and Y. Sekine, *Solid State Commun.*, 2018, **270**, 45–49.
29 S. Ø. Stub, E. Vøllestad and T. Norby, *J. Phys. Chem. C*, 2017, **121**, 12817–12825.
30 S. Ø. Stub, E. Vøllestad and T. Norby, *J. Mater. Chem. A*, 2018, **6**, 8265–8270.
31 Y. Hisai, K. Murakami, Y. Kamite, Q. Ma, E. Vøllestad, R. Manabe, T. Matsuda, S. Ogo, T. Norby and Y. Sekine, *Chem. Commun.*, 2020, **56**, 2699–2702.
32 K. Mori, N. Hashimoto, N. Kamiuchi, H. Yoshida, H. Kobayashi and H. Yamashita, *Nat. Commun.*, 2021, **12**, 3884.
33 F. Yang, B. Hu, W. Xia, B. Peng, J. Shen and M. Muhler, *J. Catal.*, 2018, **365**, 55–62.
34 W. C. Conner and J. L. Falconer, *Chem. Rev.*, 1995, **95**, 759–788.
35 J. Bigeleisen, *J. Chem. Phys.*, 1949, **17**, 675–678.
36 T. Scherban, W. K. Lee and A. S. Nowick, *Solid State Ionics*, 1988, **28-30**, 585–588.
37 T. Scherban, Y. Baikov and E. Shalkova, *Solid State Ionics*, 1993, **66**, 159–164.
38 N. Sakai, K. Yamaji, T. Horita, H. Yokokawa, Y. Hirata, S. Sameshima, Y. Nigara and J. Mizusaki, *Solid State Ionics*, 1999, **125**, 325–331.
39 Y. Nigara, K. Kawamura, T. Kawada, J. Mizusaki and M. Ishigame, *J. Electrochem. Soc.*, 1999, **146**, 2948–2953.